

# Strong yet Tough Catalyst-Free Transesterification Vitrimer with Excellent Fire-Retardancy, Durability, and Closed-Loop Recyclability

Guofeng Ye, Siqi Huo,\* Cheng Wang, Qi Zhang, Hao Wang, Pingan Song,\* and Zhitian Liu\*

Despite great advances in vitrimer, it remains highly challenging to achieve a property portfolio of excellent mechanical properties, desired durability, and high fire safety. Thus, a catalyst-free, closed-loop recyclable transesterification vitrimer (TPN<sub>1.50</sub>) with superior mechanical properties, durability, and fire retardancy is developed by introducing a rationally designed tertiary amine/phosphorus-containing reactive oligomer (TPN) into epoxy resin (EP). Because of strong covalent interactions between TPN and EP and its linear oligomer structure, as-prepared TPN<sub>1.50</sub> achieves a tensile strength of 86.2 MPa and a toughness of 6.8 MJ m<sup>-3</sup>, superior to previous vitrimer counterparts. TPN<sub>1.50</sub> containing 1.50 wt% phosphorus shows desirable fire retardancy, including a limiting oxygen index of 35.2% and a vertical burning (UL-94) V-0 classification. TPN<sub>1.50</sub> features great durability and can maintain its structure integrity in 1 M HCl or NaOH solution for 100 days. This is because the tertiary amines are anchored within the cross-linked network and blocked by rigid P-containing groups, thus effectively suppressing the transesterification. Owing to its good chemical recovery, TPN<sub>1.50</sub> can be used as a promising resin for creating recyclable carbon fiber-reinforced polymer composites. This work offers a promising integrated method for creating robust durable fire-safe vitrimers which facilitate the sustainable development of high-performance polymer composites.

polymer composites or adhesives in the areas of electric equipment, construction, traffic, and aerospace due to its superior electrical insulation, mechanical strength, and chemical and physical durability.<sup>[1]</sup> However, these thermosetting resins are extremely difficult to recycle for their stable covalently cross-linked networks.<sup>[2]</sup> As a result, most end-of-life thermosetting resins tend to be incinerated or buried, usually leading to serious impacts on the earth's environment and human health.

Introducing dynamic covalent bonds (DCB, such as  $\beta$ -hydroxyl ester,<sup>[3-5]</sup> imide,<sup>[6-8]</sup> siloxane,<sup>[9,10]</sup> and disulfide<sup>[11-13]</sup>) into cross-linked networks has been proven an effective methodology to solve their inability to be recycled, since they undergo bond exchange reaction under external stimuli, for example, light, heat, and chemicals, realizing the topological rearrangement. Based on an associative exchange mechanism, these thermosetting resins are known as vitrimers, and great efforts have recently been devoted to its development.<sup>[14-16]</sup> The transesterification vitrimer based on exchangeable  $\beta$ -hydroxyl

ester bonds was first obtained by using an additional catalyst (zinc acetate) to induce the transesterification within the polymer network (see **Figure 1a**). The external catalyst, however, can leach out from the vitrimer matrix in the long-term application

## 1. Introduction

Thermosetting resins, one of the most significant polymers, are being widely applied as a resin matrix for fiber-reinforced

G. Ye, C. Wang, Q. Zhang, Z. Liu  
Hubei Engineering Technology Research Center of Optoelectronic and New Energy Materials  
School of Materials Science & Engineering  
Wuhan Institute of Technology  
Wuhan 430205, China  
E-mail: [able.ztliu@wit.edu.cn](mailto:able.ztliu@wit.edu.cn)

 The ORCID identification number(s) for the author(s) of this article can be found under <https://doi.org/10.1002/smll.202404634>

© 2024 The Author(s). Small published by Wiley-VCH GmbH. This is an open access article under the terms of the [Creative Commons Attribution License](https://creativecommons.org/licenses/by/4.0/), which permits use, distribution and reproduction in any medium, provided the original work is properly cited.

DOI: 10.1002/smll.202404634

S. Huo, H. Wang, P. Song  
Centre for Future Materials  
University of Southern Queensland  
Springfield 4300, Australia  
E-mail: [Siqi.Huo@unisq.edu.au](mailto:Siqi.Huo@unisq.edu.au); [pingan.song@unisq.edu.au](mailto:pingan.song@unisq.edu.au)

S. Huo, H. Wang  
School of Engineering  
University of Southern Queensland  
Springfield 4300, Australia

P. Song  
School of Agriculture and Environmental Science  
University of Southern Queensland  
Springfield 4300, Australia

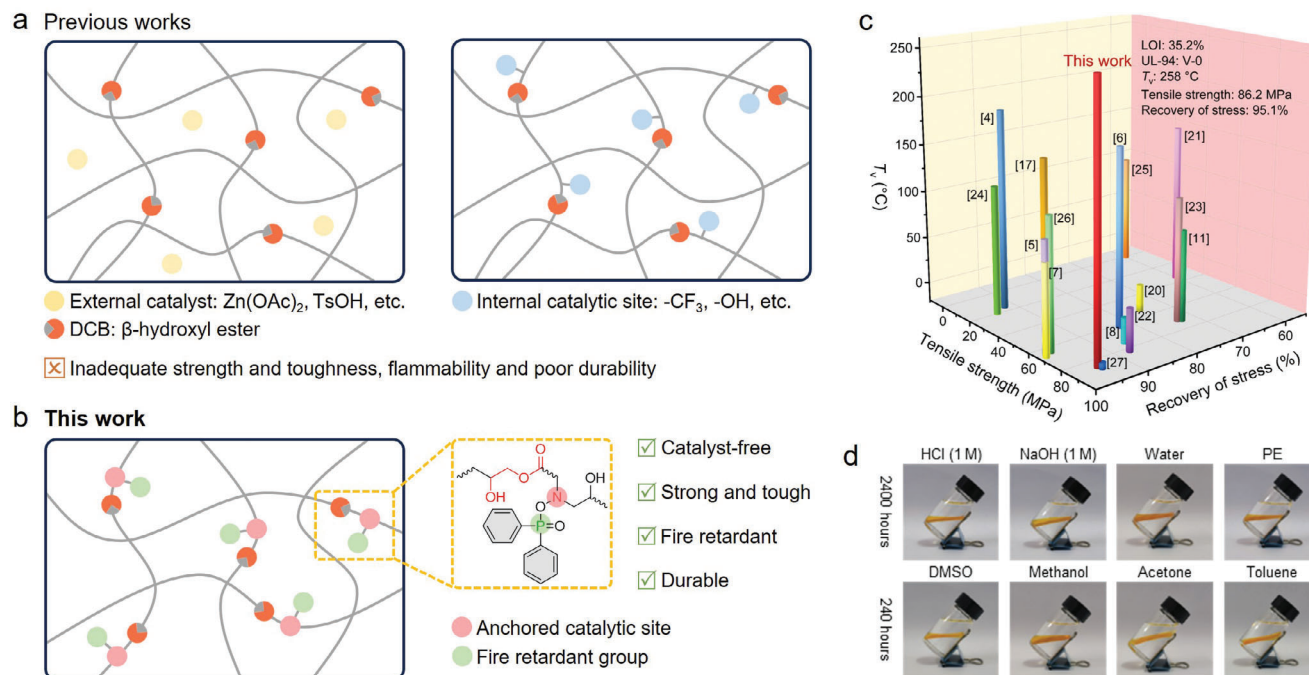


**Figure 1.** a) Illustration for the dynamic covalent networks of previous transesterification vitrimers. b) The schematic of the dynamic covalent network of  $TPN_{1.50}$  in this work. c) Comparison of the topology freeze temperature ( $T_v$ ), tensile strength, and recovery of tensile strength for previously reported vitrimers and  $TPN_{1.50}$ . d) Digital photographs of  $TPN_{1.50}$  (sample size: 30 mm  $\times$  6 mm  $\times$  2 mm) immersed in HCl (1 M), NaOH (1 M), water, petroleum ether (PE), dimethyl sulfoxide (DMSO), methanol, acetone, and toluene.

process, which can cause irreversible damage to the environment and humans.<sup>[17]</sup> Therefore, it is imperative to develop catalyst-free vitrimers. By chemically linking the  $\alpha$ - $CF_3$  groups to the  $\beta$ -hydroxyl ester-containing dynamic covalent network, a catalyst-free vitrimer was fabricated and it can be reprocessed by hot-pressing at 150 °C for 2 h.<sup>[18]</sup> The vitrimer network with both  $\beta$ -hydroxyl ester and catalytic groups can undergo topological rearrangement, thus achieving recycling and reprocessing (see Figure 1a).

In addition, the intrinsic flammability of thermosetting resins is a major barrier inhibiting their high-tech applications. The covalently introducing phosphorus-based and hydroxyl groups into a dynamic covalent network imparts flame retardancy and catalytic function to the EP system, resulting in a transesterification vitrimer with a UL-94 V-0 rating, a limiting oxygen index (LOI) of 36.0%, and the ability to be recycled at 220 °C.<sup>[19]</sup> However, these vitrimers usually suffer from unsatisfied mechanical performances, restricting industrial applications. Moreover, due to the presence of DCB, these vitrimers show poor anti-aging, chemical, and creep resistance. Therefore, it has remained a great challenge to develop advanced vitrimers with desirable mechanical properties, fire retardancy, and durability (chemical/aging/creep resistance).

To address the above challenges, a fire-retardant, catalyst-free recyclable transesterification vitrimer ( $TPN_{1.50}$ ) with superior mechanical properties and durability was prepared by covalently linking an as-synthesized tertiary amine/phosphorus-containing linear oligomer (TPN) to the EP/methyl tetrahydrophthalic anhydride (MeTHPA) network (see Figure 1b). The biphasic flame-retardant actions of P-containing groups endow

$TPN_{1.50}$  with great fire retardancy. Since the catalytic tertiary amines are fixed in the dynamic covalent network and blocked by rigid phosphorus-based groups, the resultant  $TPN_{1.50}$  shows superior chemical/aging/creep resistance, with a topology freeze temperature ( $T_v$ ) reaching 258 °C, which is higher than those of previous vitrimer counterparts (see Figure 1c).<sup>[4–8,11,17,20–27]</sup>  $TPN_{1.50}$  can maintain structural integrity after being soaked in 1 M HCl or NaOH solution for 2400 hours (see Figure 1d). In addition, the tensile strength of  $TPN_{1.50}$  is as high as 86.5 MPa because of the in situ strengthening effect of TPN (see Figure 1c).<sup>[28]</sup> The outstanding durability and mechanical robustness of  $TPN_{1.50}$  make it superior to its existing counterparts. Due to the tertiary amines chemically connecting to the vitrimer network,  $TPN_{1.50}$  can be recycled in a closed-loop, and as a polymer matrix to fabricate the advanced carbon fiber reinforced polymer (CFRP) composites, of which both matrix and carbon fibers (CFs) are chemically recyclable. Hence, this work provides a promising approach for creating high-performance epoxy vitrimers.

## 2. Results and Discussion

### 2.1. Optical and Mechanical Properties

The high transparency of EP makes it ubiquitously used in coatings, optical devices, and other fields. Therefore, the development of transparent EP vitrimers greatly contributes to their industrialization. The visible transparency of EP and TPN-containing EP ( $TPN_x$ , x was representative of its phosphorus content) vitrimers was evaluated by a visible spectrophotometer and digital camera. The visible spectra of all EP samples and the digital photo

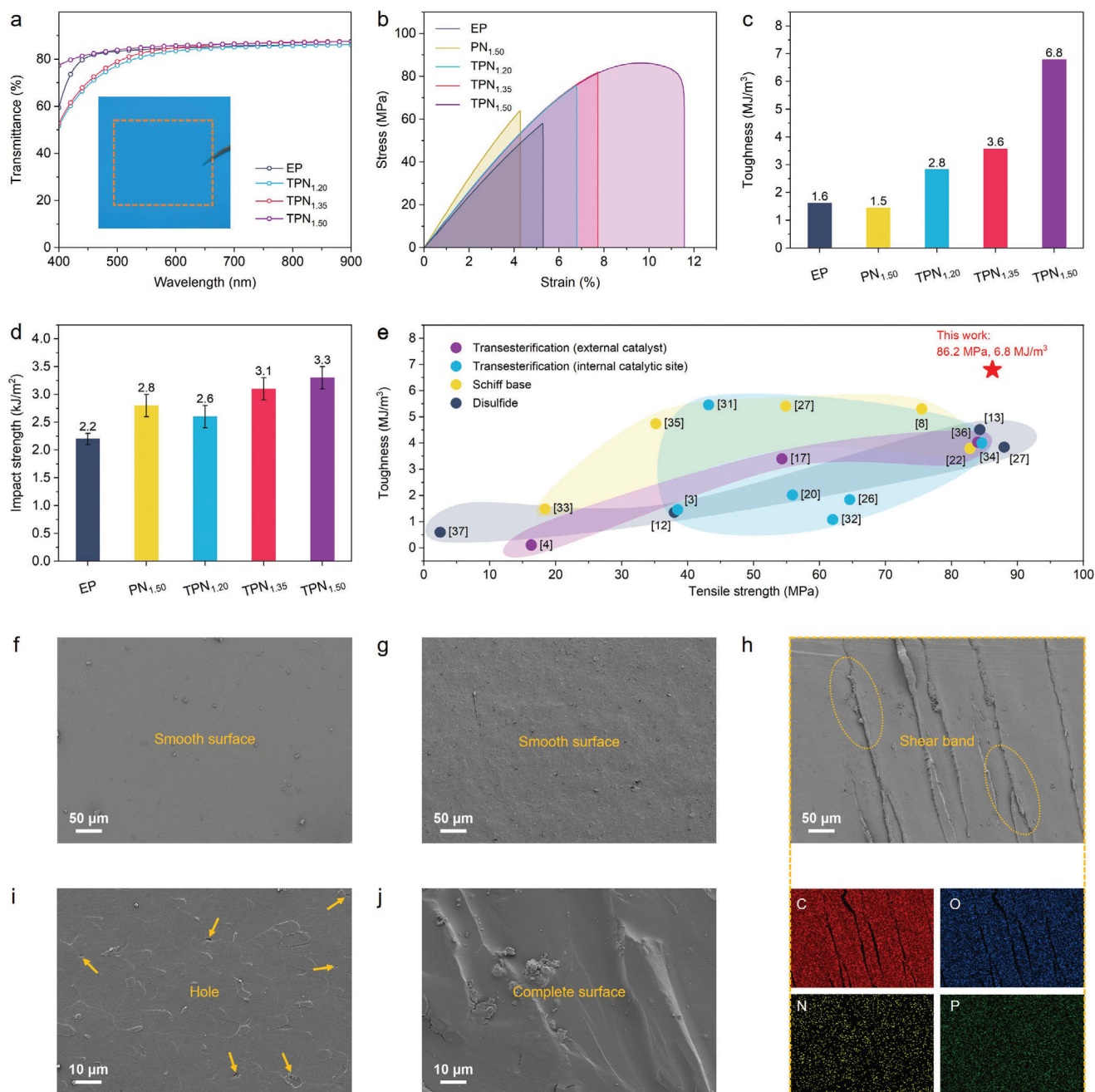


**Figure 2.** a) Visible transmission spectra of EP samples and the digital image of TPN<sub>1.50</sub> (film size: 50 mm × 50 mm × 0.2 mm). b) Tensile stress–strain curves, c) toughness, and d) impact strength of EP samples. e) Comparison of toughness and tensile strength for TPN<sub>1.50</sub> and previously reported vitrimer systems. Scanning electron microscope (SEM) images of fractured surfaces for f) EP and g) PN<sub>1.50</sub>. h) SEM image and elemental mappings of fractured surface for TPN<sub>1.50</sub>. SEM images of fractured surfaces for i) PN<sub>1.50</sub> and j) TPN<sub>1.50</sub> after etching by *N,N*-dimethylacetamide for 24 h.

of TPN<sub>1.50</sub> are shown in **Figure 2a**. All TPN<sub>x</sub> vitrimers show high transparency, with their transmittance close to that of pure EP in the wavelength of 650 to 900 nm. Specifically, TPN<sub>1.50</sub> shows transmittance of 86.4% at 700 nm, which is slightly higher than 85.6% of EP. The superior optical properties of TPN<sub>x</sub> vitrimers are primarily attributed to the good compatibility between EP and TPN because of the similarity in their backbone structure and covalent interactions (see Section S3, Supporting Information). In addition, the good compatibility of EP and TPN is a crit-

ical factor for TPN<sub>x</sub> vitrimers to achieve superior comprehensive performances.<sup>[29]</sup>

The mechanical properties of EP, TPN<sub>x</sub>, and control vitrimer sample with ((bis(2-hydroxypropyl)amino)oxy)diphenylphosphine oxide (PN<sub>1.50</sub>, its phosphorus content = 1.50 wt%) were investigated in detail (see Figure S4 and Table S3, Supporting Information). Clearly, TPN<sub>x</sub> shows better mechanical performances than EP, and the mechanical properties of TPN<sub>x</sub> gradually enhance with

increasing loading level of TPN. TPN<sub>1.50</sub> displays the best mechanical properties among all TPN<sub>x</sub>, and its tensile strength ( $\sigma$ ), elongation at break ( $\delta$ ), toughness, impact strength ( $\alpha_k$ ), critical stress intensity factor ( $K_{IC}$ ) and critical energy release rate ( $G_{IC}$ ) reach 86.2 MPa, 11.6%, 6.8 MJ m<sup>-3</sup>, 3.3 kJ m<sup>-2</sup>, 1.5 MPa·m<sup>1/2</sup>, and 7.2 kJ m<sup>-2</sup>, which are 48.4, 118.9, 325.0, 50.0, 36.4, and 50.0% higher than those of EP, respectively. Notably, the  $\sigma$ ,  $\delta$ , toughness,  $K_{IC}$ , and  $G_{IC}$  of PN<sub>1.50</sub> are all much lower than those of TPN<sub>1.50</sub> and only comparable to those of EP. The toughening and strengthening effects of TPN are mainly due to its linear oligomeric structure.<sup>[28]</sup> In addition, the  $\sigma$  and toughness of TPN<sub>1.50</sub> and previous vitrimers are compared in Figure 2e.<sup>[3,4,8,12,13,17,20,22,26,27,30–37]</sup> Obviously, TPN<sub>1.50</sub> displays higher  $\sigma$  and toughness than previous vitrimers, including transesterification-, Schiff base-, and disulfide-based, demonstrating that introducing our rationally designed reactive oligomer into EP vitrimers can break the trade-off between strength and toughness.

Additionally, the dynamic mechanical properties of EP samples were investigated by dynamic mechanical analysis (DMA). The crosslink density ( $\rho$ ) of EP samples is determined by the classical theory of rubber (see Section S1.5, Supporting Information).<sup>[38]</sup> The storage modulus ( $E'$ ) and tan delta plots and resulting data are presented in Figure S4c,d and Table S3 (Supporting Information). The introduction of TPN results in significantly increased  $E'$  values (at 30 °C) of TPN<sub>x</sub> relative to that of EP, indicating that the introduction of TPN improves the rigidity of epoxy vitrimers.<sup>[39]</sup> The glass transition temperature ( $T_g$ ) of TPN<sub>x</sub> samples is lower than that of EP. It is attributed to the introduction of linear oligomeric TPN, which reduces the crosslinking density of epoxy vitrimers. Notably, TPN<sub>1.50</sub> demonstrates the highest  $T_g$  and  $\rho$  among all TPN<sub>x</sub> samples, which is mainly due to the chemical reaction of abundant hydroxyl groups in TPN with the EP matrix (see Section S3, Supporting Information). Besides strength and toughness, TPN can dramatically enhance the rigidity of epoxy vitrimers.

The morphology of the fracture surface for EP specimens was characterized by SEM to explore the toughening and strengthening mode of action for TPN. The micrographs of the cross-sections for the EP, PN<sub>1.50</sub>, and TPN<sub>1.50</sub> specimens after Izod impact tests are illustrated in Figure 2f–h. The EP and PN<sub>1.50</sub> samples show smooth fracture surfaces, reflecting their mode of brittle fracture. However, the cross-section of TPN<sub>1.50</sub> is rough in the presence of TPN. In addition, within the fractured surface of TPN<sub>1.50</sub>, numerous shear bands are detected. Furthermore, both nitrogen and phosphorus atoms are homogeneously dispersed in the fractured surface of TPN<sub>1.50</sub>, which is consistent with the results of transparency, further confirming a good compatibility between EP and TPN. The formation of shear bands indicates the in situ toughening and strengthening effects of the well-dispersed TPN.<sup>[38,40]</sup> To further characterize the microstructures of PN<sub>1.50</sub> and TPN<sub>1.50</sub>, their fractured surfaces were etched with *N,N*-dimethylacetamide (DMAc) for 24 h. After the evaporation of solvent, the fractured surfaces were investigated with SEM, and the results are listed in Figure 2i,j. The etched cross-section of PN<sub>1.50</sub> shows distinguishable holes, which suggests that small PN molecules suffer from poor interactions with the epoxy matrix, resulting in inferior mechanical properties.<sup>[41]</sup> In contrast, there are insignificant holes or phase-separated structures on the

etched fracture surface of TPN<sub>1.50</sub>. This phenomenon indicates that the reactive, oligomeric TPN forms strong covalent interactions with the epoxy matrix to resist solvent etching.<sup>[28]</sup> When the EP matrix is subjected to external forces, the strong covalent interaction of TPN with the matrix resists further crack propagation and dissipates lots of energy. In conclusion, the linear TPN can form strong covalent interactions with the EP matrix, thus adjusting the crosslinking density and the flexible nature of the vitrimer network, and effectively enhancing the robustness, stiffness, and toughness.

## 2.2. Flame-Retardant Performances and Mode of Action

LOI and UL-94 tests were conducted on EP, PN<sub>1.50</sub> and TPN<sub>x</sub>, with data presented in Figure 3a. The EP is flammable, as reflected by a low LOI of 19.2%, and fails to pass the desired UL-94 V-0 rating. With the addition of TPN, both LOI and UL-94 ratings are dramatically improved. Specifically, the TPN<sub>1.20</sub> achieves an LOI of 32.4% and passes a UL-94 V-1 rating. The TPN<sub>1.50</sub> passes a UL-94 V-0 with a high LOI of 35.2% when the phosphorus content further increases to 1.50 wt%. In addition, PN<sub>1.50</sub> containing the same P content as TPN<sub>1.50</sub> also achieves an LOI of 34.6% with a UL-94 V-0 rating. The results indicate that the P element plays a critical role in enhancing the fire retardancy of EP vitrimers. To probe the combustion behaviors of EP and TPN<sub>x</sub>, the cone calorimetry test (CCT) was carried out.<sup>[3,42]</sup> with the obtained results illustrated in Figure 3b,c and Table S4 (Supporting Information). With the addition of TPN, the heat release of EP vitrimers is decreased dramatically. Specifically, the peak heat release rate (PHRR) and total heat release (THR) of TPN<sub>1.50</sub> reduce to 433.4 kW m<sup>-2</sup> and 57.0 MJ m<sup>-2</sup>, with 45.0% and 31.5% decreases relative to those of EP. The time to ignition (TTI) of the TPN<sub>x</sub> samples is shortened due to the pyrolysis of the phosphorus-containing groups at relatively lower temperatures.<sup>[43]</sup> The average effective heat of combustion (AEHC) is used to evaluate the intensity of the combustion for gas-phase volatiles.<sup>[44]</sup> The AEHC of TPN<sub>1.50</sub> drops from 22.1 MJ kg<sup>-1</sup> of EP to 14.9 MJ kg<sup>-1</sup> by 48.3% (see Table S4, Supporting Information). Evidently, the radical-quenching effect of the P-containing decomposition fragments from TPN is responsible for the reduced gas-phase combustion of the matrix. In addition, the TPN<sub>x</sub> vitrimer shows significantly improved residual weight at flameout (RWF) than EP (see Table S4, Supporting Information). Specifically, the RWF of TPN<sub>1.50</sub> increases from 4.6% of EP to 10.8%, with a 134.8% enhancement. Therefore, TPN facilitates the charring of the EP matrix during burning, which is in accordance with the results obtained by thermogravimetric analysis (TGA) (see Section S4, Supporting Information). Meanwhile, the denseness and degree of expansion of TPN<sub>1.50</sub> char are remarkably improved in comparison with those of EP char (see Figure 3f), which further indicates the protection effect of TPN<sub>1.50</sub> char.<sup>[45]</sup> The flame-retardant mode of action can be divided into three parts: flame inhibition effect (FIE), charring effect (CE), and barrier and protective effect (BPE).<sup>[46,47]</sup> The FIE is related to the gaseous-phase flame retardancy, and the CE and BPE are related to the condensed-phase flame retardancy. The FIE, CE, and BPE values of EP samples are listed in Table S4 (Supporting Information). The FIE value is increased with the

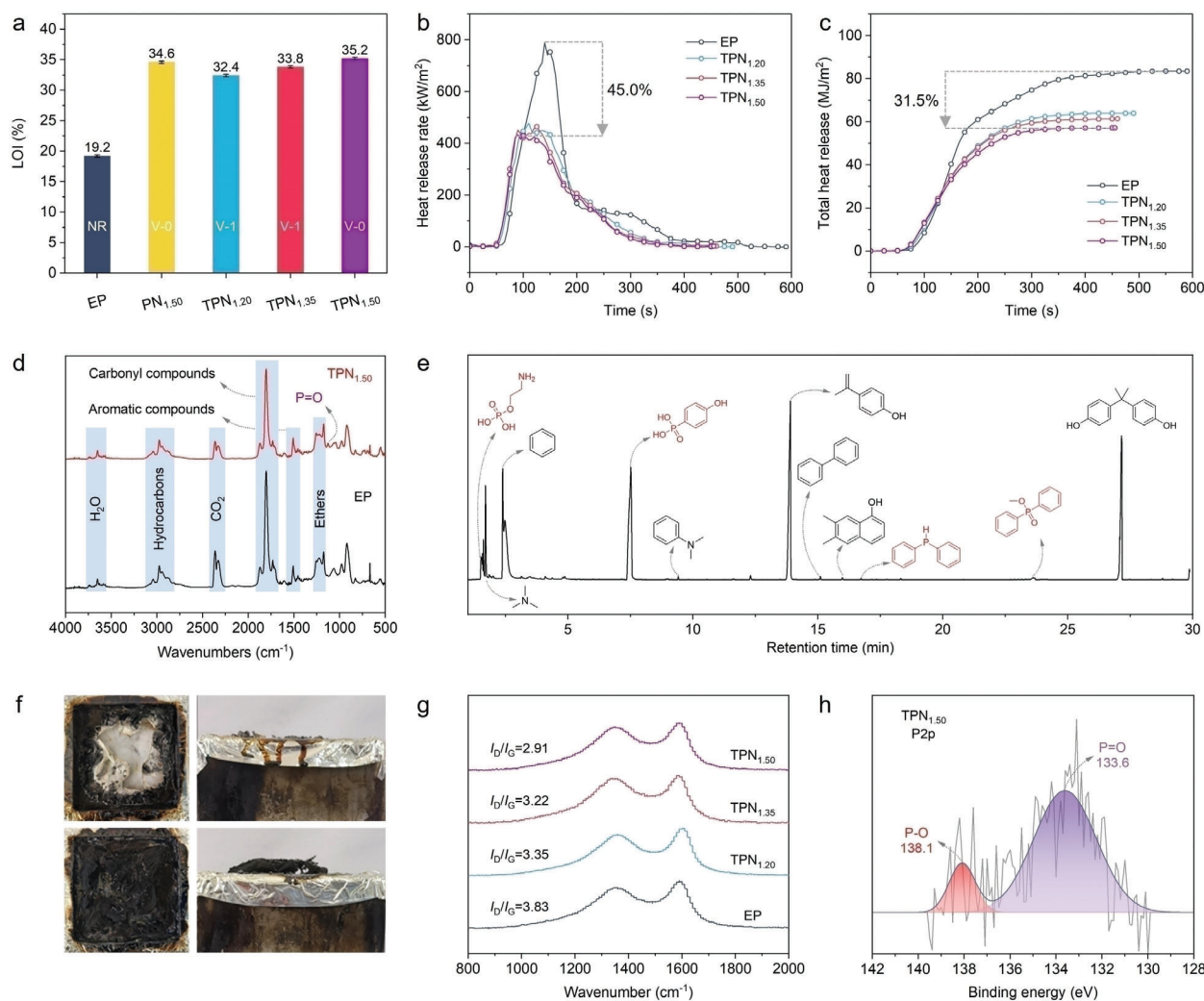


**Figure 3.** a) LOI and UL-94 results of EP samples. b) Heat release rate curves and c) total heat release plots of EP samples. d) FTIR of the pyrolysis products of EP and TPN<sub>1.50</sub> at  $T_{max}$ . e) Total ion chromatogram of TPN. f) Top- and side-view digital images of residual chars for EP and TPN<sub>1.50</sub>. g) Raman spectra of residual chars for EP samples. h) High-resolution XPS P2p spectra of residual char for TPN<sub>1.50</sub>.

increasing phosphorus content, demonstrating the gradual enhancement in the gas-phase flame-retardant effect. Additionally, the BPE values of TPN<sub>x</sub> are in high levels, which are  $\approx 20\%$ . In combination with the residual char results from TGA and CCT, TPN also functions in a condensed phase during combustion by a barrier/protective effect. In sum, TPN acts in both gas and condensed phases via flame inhibiting and barrier/protective effects to suppress the combustion, thus enhancing flame retardancy.

Thermogravimetric analysis-infrared spectrometry (TG-IR) and Pyrolysis-gas chromatography/mass spectrometry (Py-GC/MS) tests were employed to investigate the gas-phase mode-of-action.<sup>[48,49]</sup> First, the Fourier transform infrared spectroscopy (FTIR) of the decomposition volatiles for EP and TPN<sub>1.50</sub> at the temperature of the maximum weight loss rate ( $T_{max}$ ) is shown in Figure 3d. Their decomposition products are similar and consist mainly of ethers (1175  $\text{cm}^{-1}$ ), aromatic compounds (1510  $\text{cm}^{-1}$ ), carbonyl compounds (1805  $\text{cm}^{-1}$ ), CO<sub>2</sub> (2365  $\text{cm}^{-1}$ ), hydrocarbons (2975  $\text{cm}^{-1}$ ) and water (3650  $\text{cm}^{-1}$ ). Notably, all absorption intensities of these characteristic

peaks for TPN<sub>1.50</sub> are lower than those for EP (see Figures S5 and S6, Supporting Information). Hence, the decomposition products of TPN greatly suppress the thermal decomposition and facilitate the charring of the EP matrix during burning. Furthermore, a new peak of P=O is observed at 1128  $\text{cm}^{-1}$  from TPN<sub>1.50</sub> (see Figure 3d).<sup>[50]</sup> It confirms the generation of the P-containing fragments from TPN, which can further decompose into P-containing radicals to suppress gas-phase burning by quenching the high-energy radicals derived from the EP matrix. Moreover, the total ion chromatogram of TPN and the major pyrolysis products are summarized in Figure 3e and Table S5 (Supporting Information). The amine-based organics, phosphorus-containing fragments, and aromatic derivatives are the main pyrolysis products of TPN. In the initial pyrolysis stage, the nitrogen-containing fragments are released at the retention time of 1.53, 1.62, 4.10, 8.98, and 9.41 min due to the presence of weak C–N bonds. Along with the release of nitrogen-containing fragments, abundant phosphorus-containing and aromatic organics are generated, which further indicates that

the diphenylphosphine oxide group pyrolyzes to release P-containing radicals with a radical-quenching effect after cleavage from the backbone of TPN.<sup>[51,52]</sup> Based on the above results, the release of phosphorus-based radicals is responsible for the reduced gas-phase burning degree of TPN<sub>x</sub>.

To characterize the condensed-phase mode-of-action, Raman spectroscopy and X-ray photoelectron spectroscopy (XPS) were carried out to investigate the degree of graphitization, chemical composition, and bonding state of the EP residual char from CCT.<sup>[53]</sup> The residual chars display the D and G bands at 1360 and 1605 cm<sup>-1</sup>, belonging to the amorphous carbon and graphite structures, respectively (see Figure 3g). The integral area ratio of the D-band to the G-band ( $I_D/I_G$ ) is directly related to the graphitization degree of char.<sup>[54]</sup> With increasing phosphorus content, the  $I_D/I_G$  value of residual char monotonically decreases, indicative of an increased degree of graphitization. Hence, the decomposition products of TPN facilitate the charring of EP and increase the degree of graphitization of the residual char during combustion, which inhibits heat release and oxygen transfer. Additionally, the char of EP includes the C (76.31 wt%), N (1.58 wt%), and O (22.11 wt%) elements (see Table S6, Supporting Information). In the C1s spectrum of EP char, three deconvolution peaks belonging to C=O, C—O/C—N, and C—C/C—H are detected. In the N1s spectrum, two peaks attributed to N—C and N—H appear, and in the O1s spectrum, two deconvolution peaks assigned to O—C and O=C are observed (see Figure S7a–c, Supporting Information).<sup>[55]</sup> In addition to the above elements, the P (0.86 wt%) element can be detected in the char of TPN<sub>1.50</sub> (see Figure 3h; Figure S7d–f, Supporting Information). In addition, both P—O and P=O groups are identified in the P2p spectrum of TPN<sub>1.50</sub> char, indicating that the condensed-phase decomposition products of TPN are the phosphate derivatives. Meanwhile, the C content of TPN<sub>1.50</sub> char increases from 76.31 wt% of EP char to 78.66 wt%, which implies that the decomposition products of P-containing groups for TPN have reacted with the carbon-containing groups in EP during burning, leading to an increased carbon content. In summary, the P-containing decomposition products of TPN catalyze the EP matrix to form a compact and expanded char with a high graphitization degree on its surface during burning, which can impede the transfer of heat and protect the underlying substrate. Meanwhile, the phosphorus-based radicals derived from TPN trap the active radicals produced by the degradation of the EP substrate, inhibiting the combustion in the gas phase. Therefore, the superior fire retardance of TPN<sub>x</sub> vitrimers is mainly due to the bi-phase modes of action of the phosphorus-containing groups in TPN.

### 2.3. Aging/Solvent/Creep Resistance

Due to the dynamic covalent networks of vitrimers, they are usually susceptible to aging, solvent, and creep, significantly restricting their practical applications.<sup>[56–58]</sup> To assess the antiaging of TPN<sub>x</sub>, the accelerated aging tests were performed on both TPN<sub>1.50</sub> and PN<sub>1.50</sub> under different conditions (80 °C deionized water for 7 days; 100 °C oven for 7 days; 1 M HCl for 36 h; 1 M NaOH for 36 h; and UV light for 7 days), with the results presented in Figures 4a–f and S8 (Supporting Informa-

tion). The transparency and morphology of PN<sub>1.50</sub> and TPN<sub>1.50</sub> are preserved after various aging tests (see Figure S8, Supporting Information). Remarkably, the UL-94 classification of PN<sub>1.50</sub> is reduced from V-0 to V-1 after different accelerated-aging testing, while that of TPN<sub>1.50</sub> is unchanged (see Table S7, Supporting Information). Moreover, TPN<sub>1.50</sub> exhibits much lower mass loss, reduction of tensile strength, and reduction of LOI than PN<sub>1.50</sub> after different kinds of aging tests, indicative of superior environmental stability (see Figure 4a–f). Also, the solvent resistance tests of PN<sub>1.50</sub> and TPN<sub>1.50</sub> were conducted, with the results shown in Figure 1c and Figure S9 (Supporting Information). TPN<sub>1.50</sub> can effectively maintain its structure integrity for more than 240 h in various polar and non-polar solvents, for example, water, DMSO, methanol, acetone, tetrahydrofuran (THF), ethyl acetate (EA), trichloromethane (TM), toluene, and PE, and for more than 2,400 h in 1 M HCl or 1 M NaOH solution. However, PN<sub>1.50</sub> swells and degrades after a short immersion in these solvents. These results demonstrate that TPN<sub>1.50</sub> shows better solvent resistance than PN<sub>1.50</sub>.

The creep time-temperature superposition (TTS) plots of PN<sub>1.50</sub> and TPN<sub>1.50</sub> are shown in Figure 4g,h. For PN<sub>1.50</sub> and TPN<sub>1.50</sub>, the temperatures at which creep strain is lower than 1.0% are 70 and 80 °C, and the break temperatures are 90 and 100 °C. TPN<sub>1.50</sub> features superior creep resistance to PN<sub>1.50</sub>. In addition, the stress relaxation curves for TPN<sub>1.50</sub> are reported in Figure S10 (Supporting Information). TPN<sub>1.50</sub> shows stress relaxation at high temperatures, and its G/G<sub>0</sub> value can only reduce to 0.6 at 200 °C for 10<sup>4</sup> s, further indicating that TPN<sub>1.50</sub> has good dimensional stability. In fact, the G/G<sub>0</sub> value of TPN<sub>1.50</sub> cannot be reduced to 1/e at high temperatures, and thus the thermal expansion method was selected to determine the T<sub>v</sub> of TPN<sub>1.50</sub> (see Figure 4i). The T<sub>v</sub> of TPN<sub>1.50</sub> reaches 258 °C, which is 36 °C higher than that of PN<sub>1.50</sub> (222 °C), further confirming its better creep resistance. The T<sub>v</sub> of TPN<sub>1.50</sub> is also compared with those of previously reported vitrimers in Figure 1 and Table S8 (Supporting Information). TPN<sub>1.50</sub> exhibits a greater thermal dimensional stability than PN<sub>1.50</sub>, as reflected by a higher T<sub>v</sub>. These results confirm that chemically anchoring the catalytic sites (tertiary amines) into the backbone of the transesterification vitrimer network can restrict its migration and catalytic activity, thus endowing the vitrimer with superior aging, solvent, and creep resistance. In addition, Gibbs free energy was calculated through simplified chemical models to investigate the effect of the neighboring group for tertiary amine on its catalytic activity toward transesterification reaction (see Figure 4j; Figure S11, Supporting Information). Three simplified reaction models were developed, including 2-hydroxypropyl acetate (HA) + simplified TPN (STPN), HA + ((bis(2-hydroxypropyl)amino)oxy)diphenylphosphine oxide (PN), and HA + N-methyl diisopropanolamine (NA). The HA + STPN system shows the highest barrier potential in the first and second transition states among the three reaction models, demonstrating its lowest reactivity. This also implies that the rigidity of the neighboring groups for the tertiary amine plays an important role in its catalytic effect toward transesterification reactions.<sup>[59]</sup> In conclusion, it is the anchoring effect of the tertiary amines within the crosslinking network and the blocking effect of rigid phosphorus-containing groups on the amine groups that contribute to enhanced durability (aging, chemical, and creep resistance) of epoxy vitrimers.

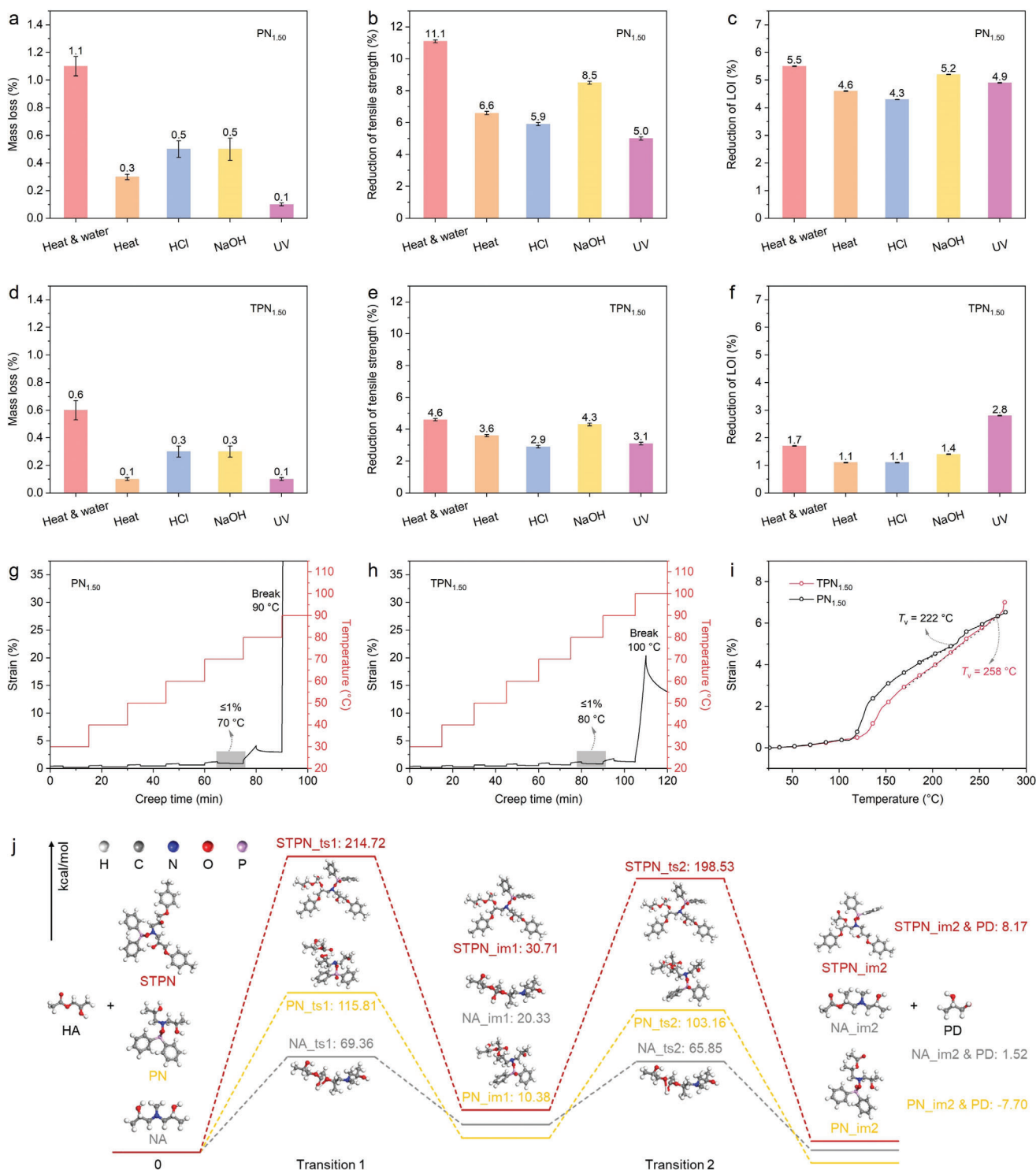


**Figure 4.** Mass loss of a)  $PN_{1.50}$  and d)  $TPN_{1.50}$  after different accelerated-aging tests. Reduction of tensile strength for b)  $PN_{1.50}$  and e)  $TPN_{1.50}$  after different accelerated-aging tests. Reduction of LOI for c)  $PN_{1.50}$  and f)  $TPN_{1.50}$  after different accelerated-aging tests. Creep time-temperature superposition curves of g)  $PN_{1.50}$  and h)  $TPN_{1.50}$ . i) Thermal expansion curves of  $PN_{1.50}$  and  $TPN_{1.50}$  from DMA. j) Calculation of the Gibbs free energy of the transesterification reaction of different simplified models by density functional theory (DFT).

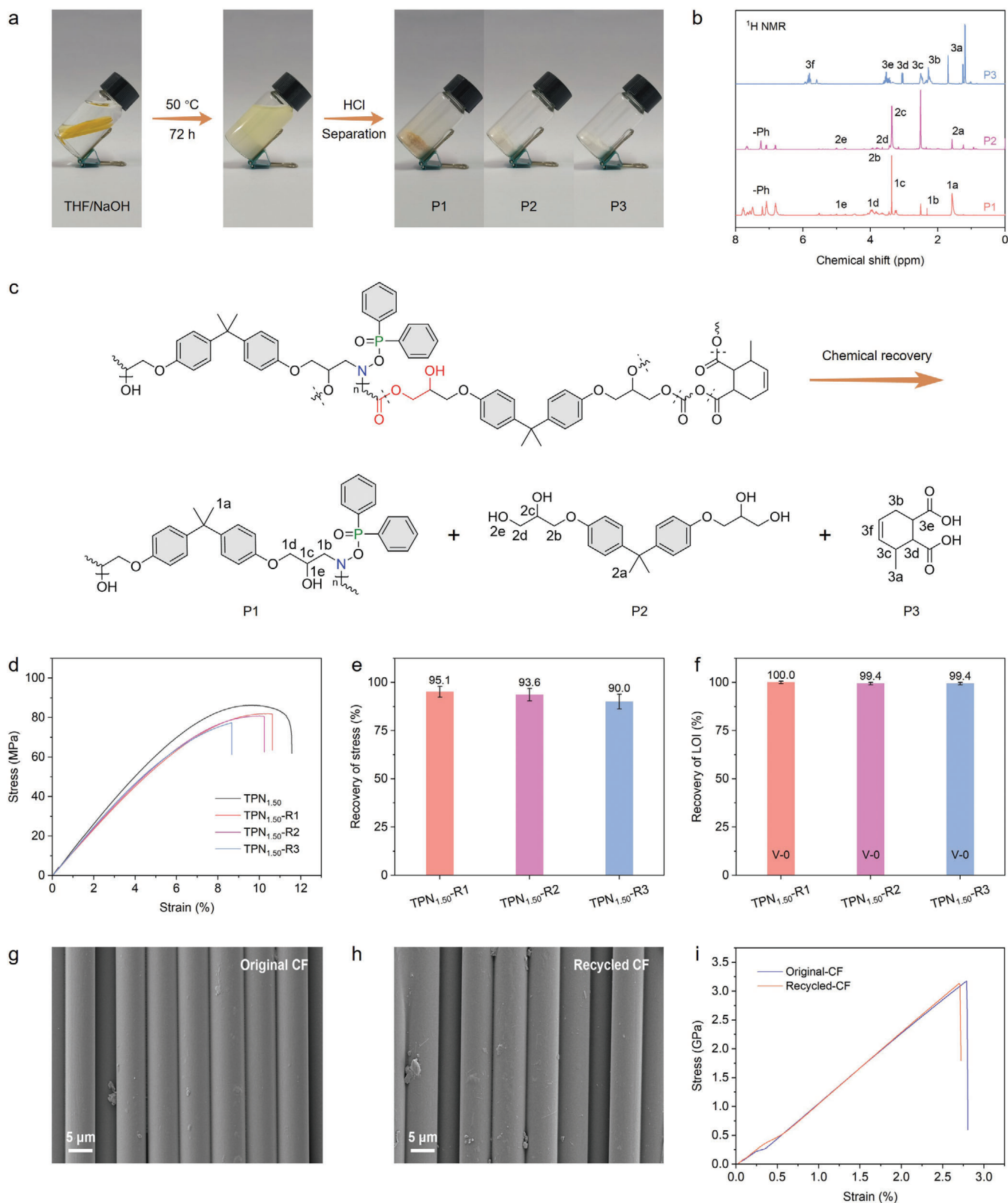


**Figure 5.** a) Chemical recovery process for TPN<sub>1.50</sub>. b)  $^1\text{H NMR}$  of the chemically recovered compounds (P1, P2, and P3). c) Possible recycling mechanisms for TPN<sub>1.50</sub>. d) Tensile stress–strain curves of TPN<sub>1.50</sub>, TPN<sub>1.50</sub>-R1, TPN<sub>1.50</sub>-R2, and TPN<sub>1.50</sub>-R3. e) Recovery of tensile strength for TPN<sub>1.50</sub>-R1, TPN<sub>1.50</sub>-R2, and TPN<sub>1.50</sub>-R3. f) Recovery of LOI for TPN<sub>1.50</sub>-R1, TPN<sub>1.50</sub>-R2, and TPN<sub>1.50</sub>-R3. SEM images of g) original and h) recycled CFs. i) Tensile stress–strain curves of original and recycled CFs.

## 2.4. Chemical Recovery

Because of the dynamic features, vitrimer can normally be repaired, reprocessed, and recycled by topological rearrangement of its dynamic covalent network under external stimuli, such as light, heat, and chemicals. These features make the vitrimer one promising polymer matrix for manufacturing CFRP composite because of its recyclability. For CF-reinforced vitrimer composites, the chemical recovery method is more suitable than the physical one (by heat) since it can recycle both polymer monomers and CFs. Hence, the chemical recycling of TPN<sub>1.50</sub> was first investigated. Initially, the chemical degradation process was investigated by characterizing the degradation products of TPN<sub>1.50</sub>. As displayed in Figure 5a, it completely degraded in THF/NaOH (volume ratio = 8:2) at 50 °C for 72 h. The obtained solution was neutralized with 1 M HCl until its pH value reached 7. After the removal of solvent, the resultant products were separated by column chromatography as P1, P2, and P3. Taking P1 as an example, the <sup>31</sup>P nuclear magnetic resonance (NMR) of P1 shows a single shift at 31.0 ppm (see Figure S12, Supporting Information). In the <sup>1</sup>H NMR spectrum of P1 (see Figure 5b), the chemical shifts near 6.7 to 7.8 ppm are assigned to the benzene protons; the shifts ≈ 5.0 ppm are attributed to the proton of —OH; the shifts between 3.7 to 4.3 ppm correspond to the protons of —O—CH<sub>2</sub>—; and the chemical shifts ≈ 3.3 and 2.3 ppm belong to the protons of —CH— and —N—CH<sub>2</sub>—, respectively. Notably, the chemical shift of P1 at 1.6 ppm is assigned to the protons of —CH<sub>3</sub>— from the bisphenol A-derived group. These results suggest that P1 is a TPN derivative (see Figure 5c). In addition, P2 and P3 are found to be bisphenol A-bis(2,3-dihydroxypropyl) ether and methyltetrahydrophthalic acid by analyzing their <sup>1</sup>H NMR (see Figure 5b), which are the derivatives of DGEBA and MeTHPA, respectively (see Figure 5c). Hence, TPN<sub>1.50</sub> can be chemically degraded into two monomers and one oligomer by the hydrolysis of its ester groups (see Figure 5c) in a mild condition. The resultant P1, P2, and P3 can also be applied to regenerate the TPN<sub>1.50</sub> vitrimer by mixing in *N,N*-dimethylformamide (DMF) at 80 °C, removing DMF under reduced pressure, and hot-pressing at 150 °C under 5 MPa for 2 h. The re-formed TPN<sub>1.50</sub> is denoted as TPN<sub>1.50</sub>-R<sub>y</sub>, where *y* represents the recovery times. As shown in Figure 5d–f and Table S9 (Supporting Information), the TPN<sub>1.50</sub>-R<sub>y</sub> maintains the mechanical and flame-retardant properties of the original TPN<sub>1.50</sub>. The recovery of tensile strength for TPN<sub>1.50</sub>-R3 after three chemical recycling cycles reaches 90.0%, and the recovery of LOI is as high as 99.4% (the recovery calculation methods listed in Section S1.5, Supporting Information), and the recycled TPN<sub>1.50</sub> still passes a UL-94 V-0 rating. Thus, TPN<sub>1.50</sub> is a closed-loop recyclable vitrimer. In addition, the recyclability of TPN<sub>1.50</sub> vitrimer is better than that of PN<sub>1.50</sub> vitrimer in terms of recovery of the tensile strength (see Tables S9 and S10, Supporting Information).

Additionally, the TPN<sub>1.50</sub> vitrimer was used as a resin matrix for manufacturing recyclable CFRP composites. The CFs can be fully recovered by dissolving the TPN<sub>1.50</sub> matrix of the composite in the THF/NaOH solution (see Figure S13, Supporting Information). The recycled CFs have a similar surface morphology to the original CFs, and no polymer matrix is left on the recycled CF surface (see Figure 5g,h). To quantitatively analyze the performances of the recycled CF, the single-fiber tensile tests were performed on

both original and recycled CFs. The tensile strength and elongation at the break of the recycled CF are 3.1 GPa and 2.7%, respectively, close to 3.2 GPa and 2.8% of the original CF (see Figure 5i; Table S11, Supporting Information). Hence, the TPN<sub>1.50</sub> vitrimer can be recycled in a closed-loop chemical manner and reused many times (at least 3 times), which shows broad application prospects in the creation of advanced recyclable CFRP composites.

## 3. Conclusion

In this work, a high-performance, strong yet tough fire-safe TPN<sub>1.50</sub> vitrimer with superior durability and closed-loop, catalyst-free recyclability was developed based on a rationally designed phosphorus/tertiary amine-containing, reactive oligomer (TPN). Because the catalytic sites (tertiary amines) are anchored within the crosslinked network and blocked by rigid phosphorus-containing groups, the TPN<sub>1.50</sub> vitrimer exhibits superior chemical, anti-aging, and creep-resistant properties. The TPN<sub>1.50</sub> vitrimer features outstanding mechanical properties, with tensile strength and toughness respectively reaching 86.2 MPa and 6.8 MJ m<sup>-3</sup>, outperforming previous vitrimer counterparts. Due to the gas/condensed-phase flame-retardant action of phosphorus, the TPN<sub>1.50</sub> vitrimer shows desirable fire retardancy (LOI: 35.2% and UL-94 V-0). Importantly, the TPN<sub>1.50</sub> vitrimer can be chemically recovered up to 3 times, making it a promising polymer matrix for the fabrication of advanced, recyclable CFRP composites, in which both matrix and CFs are closed-loop recyclable. Therefore, this work provides a simple yet effective strategy for the creation of catalyst-free, closed-loop recyclable vitrimers combining exceptional mechanical, fire-retardant, and durable performances, which is expected to significantly expedite the practical application of vitrimer.

## 4. Experimental Section

This section is presented in the Supporting Information.

## Supporting Information

Supporting Information is available from the Wiley Online Library or from the author.

## Acknowledgements

This work was funded by the Australian Research Council (DE230100616, LP220100278, and DP240102628), the Foundation for Outstanding Youth Innovative Research Groups of Higher Education Institution in Hubei Province (T201706), the Foundation for Innovative Research Groups of Hubei Natural Science Foundation of China (2017CFA009), and the Foundation for 15th Graduate Education Innovation of Wuhan Institute of Technology (CX2023106).

Open access publishing facilitated by University of Southern Queensland, as part of the Wiley - University of Southern Queensland agreement via the Council of Australian University Librarians.

## Conflict of Interest

The authors declare no conflict of interest.

## Data Availability Statement

The data that support the findings of this study are available from the corresponding author upon reasonable request.

## Keywords

chemical recovery, durability, fire retardancy, mechanical properties, vitrimer

Received: June 6, 2024  
Revised: July 12, 2024  
Published online: July 31, 2024

- [1] Y. Jiang, J. Li, D. Li, Y. Ma, S. Zhou, Y. Wang, D. Zhang, *Chem. Soc. Rev.* **2024**, *53*, 624.
- [2] Z. Hu, F. Hu, L. Deng, Y. Yang, Q. Xie, Z. Gao, C. Pan, Y. Jin, J. Tang, G. Yu, W. Zhang, *Angew. Chem., Int. Ed.* **2023**, *62*, 202306039.
- [3] Y. Zhang, H. Yan, R. Yu, J. Yuan, K. Yang, R. Liu, Y. He, W. Feng, W. Tian, *Adv. Sci.* **2024**, *11*, 2306350.
- [4] J. H. Chen, J. H. Lu, X. L. Pu, L. Chen, Y. Z. Wang, *Chemosphere* **2022**, *294*, 133778.
- [5] Y. Liu, Z. Yu, B. Wang, X. Xu, H. Feng, P. Li, J. Zhu, S. Ma, *Eur. Polym. J.* **2022**, *173*, 111272.
- [6] P. Yu, H. Wang, T. Li, G. Wang, Z. Jia, X. Dong, Y. Xu, Q. Ma, D. Zhang, H. Ding, B. Yu, *Adv. Sci.* **2023**, *10*, 2300958.
- [7] Y. Liu, Z. Yu, G. Lu, W. Chen, Z. Ye, Y. He, Z. Tang, J. Zhu, *Chem. Eng. J.* **2023**, *451*, 139053.
- [8] W. Yang, H. Ding, W. Zhou, T. Liu, P. Xu, D. Puglia, J. M. Kenny, P. Ma, *Compos. Sci. Technol.* **2022**, *230*, 109776.
- [9] C. A. Tretbar, J. A. Neal, Z. Guan, *J. Am. Chem. Soc.* **2019**, *141*, 16595.
- [10] T. Debsharma, V. Amfilochiou, A. A. Wróblewska, I. De Baere, W. Van Paeppegem, F. E. Du Prez, *J. Am. Chem. Soc.* **2022**, *144*, 12280.
- [11] H. Wang, H.-C. Liu, Y. Zhang, H. Xu, B.-Q. Jin, Z.-X. Cao, H.-T. Wu, G.-S. Huang, J.-R. Wu, *Chinese J. Polym. Sci.* **2021**, *39*, 736.
- [12] F. Zhou, Z. Guo, W. Wang, X. Lei, B. Zhang, H. Zhang, Q. Zhang, *Compos. Sci. Technol.* **2018**, *167*, 79.
- [13] J.-T. Miao, M. Ge, Y. Wu, T. Y. Chou, H. Wang, L. Zheng, L. Wu, *Eur. Polym. J.* **2020**, *134*, 109805.
- [14] B. R. Elling, W. R. Dichtel, *ACS Cent. Sci.* **2020**, *6*, 1488.
- [15] M. Guerre, C. Taplan, J. M. Winne, F. E. Du Prez, *Chem. Sci.* **2020**, *11*, 4855.
- [16] N. J. Van Zee, R. Nicolaÿ, *Prog. Polym. Sci.* **2020**, *104*, 101233.
- [17] D. Montarnal, M. Capelot, F. Tournilhac, L. Leibler, *Science* **2011**, *334*, 965.
- [18] D. Berne, F. Cuminet, S. Lemouzy, C. Joly-Duhamel, R. Poli, S. Caillol, E. Leclerc, V. Ladmiral, *Macromolecules* **2022**, *55*, 1669.
- [19] J.-H. Chen, B.-W. Liu, J.-H. Lu, P. Lu, Y.-L. Tang, L. Chen, Y.-Z. Wang, *Green Chem.* **2022**, *24*, 6980.
- [20] X. Feng, G. Li, *ACS Appl. Mater. Interfaces* **2020**, *12*, 57486.
- [21] G. Li, P. Zhang, S. Huo, Y. Fu, L. Chen, Y. Wu, Y. Zhang, M. Chen, X. Zhao, P. Song, *ACS Sustainable Chem. Eng.* **2021**, *9*, 2580.
- [22] P.-X. Tian, Y.-D. Li, Y. Weng, Z. Hu, J.-B. Zeng, *Eur. Polym. J.* **2023**, *193*, 112078.
- [23] D. J. Fortman, J. P. Brutman, C. J. Cramer, M. A. Hillmyer, W. R. Dichtel, *J. Am. Chem. Soc.* **2015**, *137*, 14019.
- [24] Y. Nishimura, J. Chung, H. Muradyan, Z. Guan, *J. Am. Chem. Soc.* **2017**, *139*, 14881.
- [25] M. M. Obadia, B. P. Mudraboyina, A. Serghei, D. Montarnal, E. Drockenmüller, *J. Am. Chem. Soc.* **2015**, *137*, 6078.
- [26] Q. Chang, W. Li, L. Xiao, K. Zhang, J. Huang, Y. Wang, X. Nie, J. Chen, *Macromol. Chem. Phys.* **2023**, *224*, 2300272.
- [27] A. Ruiz de Luzuriaga, R. Martin, N. Markaide, A. Rekondo, G. Cabañero, J. Rodríguez, I. Odriozola, *Mater. Horiz.* **2016**, *3*, 241.
- [28] D. Chen, J. Li, Y. Yuan, C. Gao, Y. Cui, S. Li, H. Wang, C. Peng, X. Liu, Z. Wu, J. Ye, *Polymer* **2022**, *240*, 124518.
- [29] M. A. Rahim, M. Björnalm, T. Suma, M. Faria, Y. Ju, K. Kempe, M. Müllner, H. Ejima, A. D. Stickland, F. Caruso, *Angew. Chem., Int. Ed.* **2016**, *55*, 13803.
- [30] X.-M. Ding, L. Chen, Y.-J. Xu, X.-H. Shi, X. Luo, X. Song, Y.-Z. Wang, *ACS Sustainable Chem. Eng.* **2023**, *11*, 14445.
- [31] X. Feng, G. Li, *Chem. Eng. J.* **2021**, *417*, 129132.
- [32] Y. Liu, B. Wang, S. Ma, X. Xu, J. Qiu, Q. Li, S. Wang, N. Lu, J. Ye, J. Zhu, *Eur. Polym. J.* **2021**, *144*, 110236.
- [33] J. Liu, K. V. Bernaerts, *J. Mater. Chem. A* **2024**, *12*, 2959.
- [34] C. Hao, T. Liu, S. Zhang, W. Liu, Y. Shan, J. Zhang, *Macromolecules* **2020**, *53*, 3110.
- [35] S. Wang, S. Ma, Q. Li, W. Yuan, B. Wang, J. Zhu, *Macromolecules* **2018**, *51*, 8001.
- [36] D. Zhang, W. Cao, Z. Guo, H. Yan, Z. Fang, P. Chen, J. Li, *Polym. Degrad. Stab.* **2023**, *207*, 110234.
- [37] A. Vilanova-Pérez, S. Moradi, O. Konuray, X. Ramis, A. Roig, X. Fernández-Francos, *React. Funct. Polym.* **2024**, *195*, 105825.
- [38] J. Zhang, X. Mi, S. Chen, Z. Xu, D. Zhang, M. Miao, J. Wang, *Chem. Eng. J.* **2020**, *381*, 122719.
- [39] Z. H. Zhao, P. C. Zhao, S. Y. Chen, Y. X. Zheng, J. L. Zuo, C. H. Li, *Angew. Chem., Int. Ed.* **2023**, *135*, 202301993.
- [40] L. Zhong, Y. Hao, J. Zhang, F. Wei, T. Li, M. Miao, D. Zhang, *Macromolecules* **2022**, *55*, 595.
- [41] G. Ye, S. Huo, C. Wang, Q. Zhang, B. Wang, Z. Guo, H. Wang, Z. Liu, *Sustain. Mater. Technol.* **2024**, *39*, 00853.
- [42] Z. Ma, X. Liu, X. Xu, L. Liu, B. Yu, C. Maluk, G. Huang, H. Wang, P. Song, *ACS Nano* **2021**, *15*, 11667.
- [43] X. Wang, S. Zhou, W.-W. Guo, P.-L. Wang, W. Xing, L. Song, Y. Hu, *ACS Sustainable Chem. Eng.* **2017**, *5*, 3409.
- [44] J. Feng, Y. Lu, H. Xie, Z. Xu, G. Huang, C.-F. Cao, Y. Zhang, V. S. Chevali, P. Song, H. Wang, *ACS Sustainable Chem. Eng.* **2022**, *10*, 15223.
- [45] M. M. Velencoso, A. Battig, J. C. Markwart, B. Schartel, F. R. Wurm, *Angew. Chem., Int. Ed.* **2018**, *57*, 10450.
- [46] S. Brehme, B. Schartel, J. Goebbels, O. Fischer, D. Pospiech, Y. Bykov, M. Döring, *Polym. Degrad. Stab.* **2011**, *96*, 875.
- [47] J. Wang, L. Qian, Z. Huang, Y. Fang, Y. Qiu, *Polym. Degrad. Stab.* **2016**, *130*, 173.
- [48] C. Wang, S. Huo, G. Ye, B. Wang, Z. Guo, Q. Zhang, P. Song, H. Wang, Z. Liu, *Compos. Part B: Eng.* **2024**, *268*, 111075.
- [49] B. Hou, Y.-T. Pan, P. Song, *Microstructures* **2023**, *3*, 2023039.
- [50] G. Ye, S. Huo, C. Wang, Q. Shi, L. Yu, Z. Liu, Z. Fang, H. Wang, *Compos. Part B: Eng.* **2021**, *227*, 109395.
- [51] B. W. Liu, H. B. Zhao, Y. Z. Wang, *Adv. Mater.* **2022**, *34*, 2107905.
- [52] W. Zhang, J. Barrio, C. Gervais, A. Kocjan, A. Yu, X. Wang, M. Shalom, *Angew. Chem., Int. Ed.* **2018**, *57*, 9764.
- [53] J. Wang, J. Wang, S. Yang, X. Chen, K. Chen, G. Zhou, X. Liu, L. Xu, S. Huo, P. Song, H. Wang, *Chem. Eng. J.* **2024**, *485*, 149852.
- [54] G. Yang, W. H. Wu, Y. H. Wang, Y. H. Jiao, L. Y. Lu, H. Q. Qu, X. Y. Qin, *J. Hazard. Mater.* **2019**, *366*, 78.
- [55] F. Wei, J. Zhang, C. Wu, M. Luo, B. Ye, H. Zhang, J. Wang, M. Miao, T. Li, D. Zhang, *Macromolecules* **2023**, *56*, 5290.
- [56] M. Chen, B. B. Murphy, Y. Wang, F. Vitale, S. Yang, *Small* **2022**, *19*, 2205854.
- [57] Z. Xu, Y. Zhu, Y. Ai, D. Zhou, F. Wu, C. Li, L. Chen, *Small* **2024**, *2400520*, <https://doi.org/10.1002/sml.202400520>.
- [58] C. Yu, X. Li, X. Yang, X. Qiu, X. Zhang, Z. Chen, Y. Luo, *Small* **2024**, *20*, 2311656.
- [59] Y. Yang, M. W. Urban, *Chem. Soc. Rev.* **2013**, *42*, 7446.